Antibody affinity and concentration of convalescent sera provide context for reduced SARS-CoV-2 Omicron spike affinity of therapeutic antibodies

Sebastian Fiedler[1], Sean R. A. Devenish[1], Alexey S. Morgunov[1,2], Alison Ilsley[1], Francesco Ricci[1], Marc Emmenegger[3], Vasilis Kosmoliaptsis[4,5,6], Elitza S. Theel[7], John R. Mills[8,9], Anton M. Sholukh[10], Adriano Aguzzi[3], Akiko Iwasaki[11,12,13,14], Andrew K. Lynn[1], Tuomas P. J. Knowles[1,2,15*]

[1]Fluidic Analytics, Unit A, The Paddocks Business Centre, Cherry Hinton Road, Cambridge CB1 8DH, United Kingdom

[2]Centre for Misfolding Diseases, Yusuf Hamied Department of Chemistry, University of Cambridge, Lensfield Road, Cambridge CB2 1EW, United Kingdom

[3]Institute of Neuropathology, University of Zurich, 8091 Zurich, Switzerland

[4]Department of Surgery, University of Cambridge, Addenbrookes Hospital, Cambridge, CB2 0QQ, United Kingdom

[5]NIHR Blood and Transplant Research Unit in Organ Donation and Transplantation, University of Cambridge, Hills Road, Cambridge CB2 0QQ, United Kingdom

[6]NIHR Cambridge Biomedical Research Centre, Hills Road, Cambridge CB2 0QQ, United Kingdom

[7]Division of Clinical Microbiology, Department of Laboratory Medicine and Pathology, Mayo Clinic, Rochester, Minnesota, USA

[8]Department of Laboratory Medicine and Pathology, Mayo Clinic, Rochester, Minnesota, USA

[9]Center for MS and Autoimmune Neurology, Mayo Clinic, Rochester, Minnesota, USA

[10]Vaccine and Infectious Disease Division, Fred Hutchinson Cancer Research Center, Seattle, Washington, USA

[11]Department of Immunobiology, Yale School of Medicine, New Haven, CT 06519, USA

[12]Department of Epidemiology of Microbial Diseases, Yale School of Public Health, New Haven, CT 06510, USA

[13]Department of Molecular, Cellular and Developmental Biology, Yale University, New Haven, CT 06511, USA

[14]Howard Hughes Medical Institute, Chevy Chase, MD 20815, USA

[15]Cavendish Laboratory, Department of Physics, University of Cambridge, JJ Thomson Ave, Cambridge CB3 0HE, United Kingdom

*to whom correspondence should be addressed: tpjk2@cam.ac.uk

Abstract

The Omicron variant of SARS-CoV-2, first detected in November 2021, is rapidly becoming the dominant lineage worldwide. We assessed the affinities of two monoclonal antibodies (mAbs), casirivimab and imdevimab, to wild type, Delta and Omicron spike; to provide context, we compared the properties of these therapeutic mAbs to the affinities and concentrations of wild-type RBD specific antibodies in 74 convalescent sera. The affinities of both mAbs to wild type and Delta RBDs were in the same range as the polyclonal responses of the convalescents. Antibodies in a pooled, convalescent plasma from early 2020 retained nanomolar affinities to wild type, Delta and Omicron RBDs; however, the concentration of Omicron-specific antibodies decreased considerably. By contrast, the affinity of casirivimab to Omicron RBD decreased by factors >1000 and 600 compared with wild type and Delta RBDs, respectively. Imdevimab did not bind to Omicron at ≤10 µM. These results corroborate the finding that casirivimab and imdevimab do not prevent infection of cells by the Omicron variant.

Keywords (6)

Omicron, variants of concern, monoclonal antibodies, humoral immunity, antibody affinity, microfluidics

Introduction

The SARS-CoV-2 B.1.1.529 variant (Omicron) was first reported in Botswana and in South Africa in November 2021 and was classified as a variant of concern by the world health organization (WHO) on 26th of November 2021[1,2]. By mid-December 2021, the Omicron variant was detected in more than 30 countries and is expected to become the dominant lineage worldwide.

The Omicron variant is characterized by a large number of mutations present in the spike and nucleocapsid proteins as compared with previously discovered variants of SARS-CoV-2. Most critical for viral fitness and immune evasion are likely 34 mutations within the Omicron spike protein with 10 mutations within the N-terminal domain, 15 in the receptor binding domain (RBD), 3 related to the furin cleavage site and 6 in the S2 region (Tables S1 and S2). Of those mutations, 13 had been observed in previous variants of SARS-CoV-2 but never in a single lineage, as summarized in Tables S1 and S2. Despite this large number of mutations, Omicron still utilizes angiotensin converting enzyme (ACE2) as host receptor (referred to as wild type throughout the paper)[3].

Omicron reduces the virus neutralization efficacy of some approved or clinical-stage antibody drugs, with casirivimab/imdevimab (Regeneron) and bamlanivimab and etesevimab (Lilly) losing their ability to neutralize, although cilgavimab/tixagevimab (AstraZeneca) and sotrovimab (GSK) retained comparably high efficacies[3–8]. Virus neutralization was also strongly reduced in COVID-19 convalescent sera and in double-vaccinated individuals who had received BNT162b2, mRNA-1273, Ad26.COV2.S, ADZ1222, Sputnik V, or BBIBP-CorV[3,5,8–10]. While triple vaccinated individuals who received BNT162b2 or mRNA-1273 also showed reduced neutralization efficacy as compared with wild type SARS-CoV-2 and the Delta variant, the retained efficacies were considerably higher than for convalescent or double-vaccinated individuals[3,5,7,8]. Also, individuals who had been infected with either Delta or an earlier variant of SARS-CoV-2 and had then been vaccinated retained considerable titers of neutralizing antibodies[3,7,8].

The considerable extent to which the Omicron variant evades humoral immune responses, whether induced by infection or vaccination, is expected to cause more reinfections and breakthrough infections. Despite reports of a higher proportion of Omicron infections leading to milder disease outcomes[11–16], very high case numbers related to a more transmissible Omicron variant would still pose a significant public health risk.

Here, we use microfluidic diffusional sizing (MDS)[17–20] to measure the in-solution binding affinities of the Omicron spike RBD to casirivimab (REGN10933) and imdevimab (REGN10987) which constitute a therapeutic antibody-drug cocktail administered to reduce SARS-CoV-2 viral load and alleviate COVID-19 symptoms. Both antibodies bind wild type and Delta SARS-CoV-2 spike with high affinities and are potent virus neutralizing agents[21]. We observed greatly reduced binding affinities of both antibodies in the presence of the Omicron spike RBD compared with spike RBD of wild type and the Delta variant. The MDS-based antibody affinities determined were consistent with published virus-neutralization IC_{50} values and provide a quantitative explanation for their reduced efficacy. We also discuss casirivimab and imdevimab affinities to spike RBDs of wild type, Delta, and Omicron in the context of antibody affinity and concentration data obtained for COVID-19 convalescents by microfluidic antibody affinity profiling (MAAP)[17–20]. MAAP shows that wild type and Delta spike RBD affinities of casirivimab and imdevimab are within the affinity range typical of polyclonal anti-wild type spike RBD antibodies generated by the humoral immune response. For Omicron spike RBD, both antibodies have affinities several orders of magnitude lower than antibodies found in convalescent samples. We also utilized MAAP to analyze the antibody response against Omicron spike RBD in the working reagent for anti-SARS-CoV-2 immunoglobulin[22], a plasma pooled from individuals who recovered from COVID-19 in 2020. We observed considerable cross-reactivity to Omicron spike RBD and roughly half the concentration of binding antibodies as compared with wild type.

Results and Discussion

The binding affinities of Omicron spike RBD, Delta spike RBD, and wild type spike RBD to casirivimab and imdevimab were determined by MDS (Figure 1). To do so, equilibrium binding curves were acquired by titrating each antibody against constant concentrations of each spike RBD. The formation of RBD–antibody complexes was monitored based on an increase of the hydrodynamic radius (R_h) of the RBD species in solution.

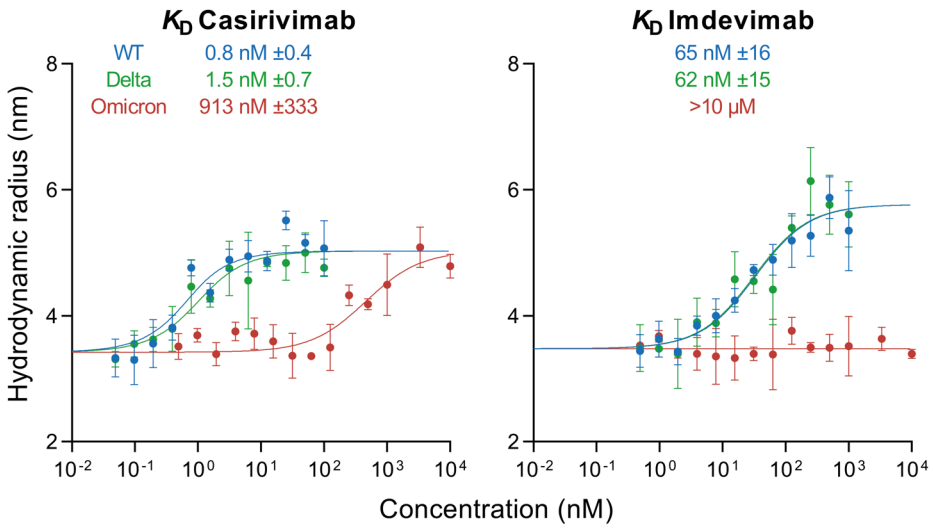

Figure 1. Equilibrium binding curves of casirivimab and imdevimab binding to spike RBD proteins from SARS-CoV-2 wild type as well as variants Delta and Omicron as determined by microfluidic diffusional sizing (MDS). Error bars are standard deviations from triplicate measurements. K_D values are best fits with standard errors from non-linear least squares fits in terms of a 2:1 binding model.

At the lowest antibody concentrations, in the absence of binding, all three types of RBD (wild type, Delta, and Omicron) displayed R_h of approx. 3.4 nm, as observed previously[17,19,20]. The complex sizes with both antibodies were as observed previously for the binding of monoclonal antibodies to spike RBD[17].

The binding affinity of both casirivimab and imdevimab was unaffected for Delta spike RBD in line with reports of only a minor reduction of virus neutralization[23]. For Omicron spike RBD, casirivimab displayed an affinity reduced by factors >1000 and 600 with respect to wild type and Delta RBDs, respectively. Imdevimab did not bind at all to Omicron spike RBD. Such drastic changes in binding affinity likely explain the inability of both antibodies to neutralize the Omicron variant[3–8]. However, the fact that casirivimab still binds to Omicron spike RBD, albeit with much reduced affinity, might render it suitable for an affinity-maturation campaign using Omicron spike as antigen.

The observation that both antibodies bound tightly to wild type spike RBD, with casirivimab binding at least an order of magnitude more tightly than imdevimab, are consistent with previous studies using SPR[21] and BLI[4]. The absolute affinities differ slightly among the three techniques perhaps due to differences in protein constructs used or technical differences such as surface immobilization in SPR and BLI versus solution measurement with MDS. Binding to Omicron RBD was studied also by BLI, which detected no binding for imdevimab, consistent with the MDS results found here. For casirivimab a sub-nanomolar affinity was determined for Omicron RBD by BLI[4], which differs strongly from the result determined by MDS showing only weak binding. Given the density of mutations in Omicron it seems likely that the affinity determined by BLI is artefactual, a possibility supported by the observation of lost neutralization efficacy for both antibodies when challenged with the Omicron variant[3–8].

The binding epitopes of both antibodies contain Omicron mutations: for casirivimab the mutations K417N, E484A, Q493R are all within 4 Å of the antibody, while imdevimab is within 4 Å of the mutations N440K and Q498R (Figure 2). The mode of action of both therapeutic antibodies is to prevent viral spike proteins from binding to ACE2[21]. While the epitope of casirivimab overlaps with the ACE2 binding site, imdevimab binds on the side of the RBD and sterically blocks ACE2 from accessing the spike protein. Together with our affinity data, this suggests that reduced antibody occupancy of viral spike proteins is the main cause for, in the case of the Delta variant, a slightly reduced neutralization efficacy, and, in the case of the Omicron variant, loss of virus neutralization ability.

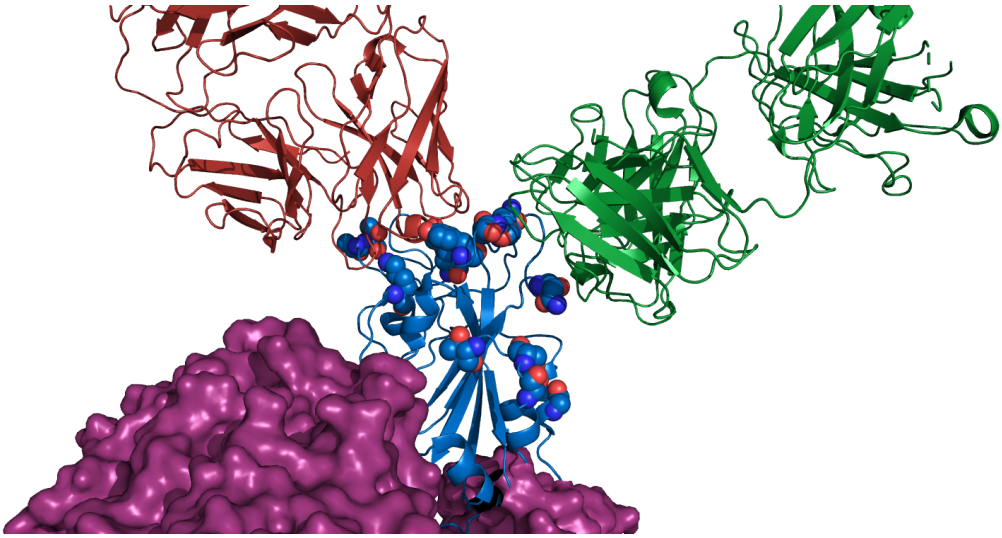

Figure 2. Structure of Fab domains of casirivimab (red) and imdevimab (green) bound to wild type RBD in the up conformation on the spike protein (purple). The residues mutated in the Omicron RBD are shown as spheres, revealing that amino acids in both antibody epitopes are mutated. The binding site of ACE2 overlaps with that of casirivimab.

Next, we analyzed how the low Omicron spike RBD binding affinities of casirivimab and imdevimab relate to polyclonal antibody responses in COVID-19 convalescent individuals (Figure 3). Generally, affinities of serum antibodies and their specific concentrations are difficult to measure. To address this issue, we recently introduced microfluidic affinity profiling (MAAP) which utilizes MDS to provide a fingerprint of the antibodies able to bind an antigen probe. Specifically, the fingerprint consists of the in-solution K_D and the concentration of antibody binding sites in any complex biological background[17–20]. To assess the functional immune response against SARS-CoV-2, MAAP is used as a new type of serological assay that allows simultaneous determination of antibody affinity against a fluorescently labeled antigen probe as well as the concentration of the binding antibodies directly in biological samples. This granular, quantitative view on the functional immune response of individuals is advantageous over commonly measured antibody titers which are a combination of both affinity and concentration. While a high titer can be achieved through either a low concentration of high affinity antibodies or a high concentration of low affinity antibodies, MAAP can readily distinguish these physiologically very distinct scenarios.

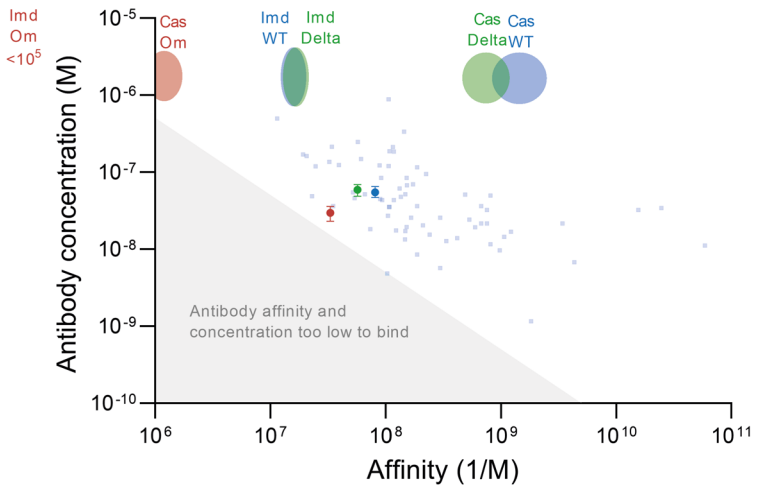

Figure 3. Affinities and average maximum post-dosage concentrations of therapeutic antibodies in comparison with affinities and concentrations of COVID-19 convalescent serum or plasma. The monoclonal antibody ovals present the affinities (K_A with standard error determined by MDS) against wild type spike RBD (blue), Delta spike RBD (green) or Omicron spike RBD (red) and maximum serum concentrations obtained after 2.4 g dose (average ± 1 SD)[24] of casirivimab (Cas) or imdevimab (Imd); see Figure 1. Light blue squares correspond to results of microfluidic antibody affinity profiling (MAAP) of convalescent serum samples collected from various cohorts of unvaccinated individuals using wild type spike RBD as antigen (see Table S3 for details). Circles correspond to MAAP performed on the working reagent for anti-SARS-CoV-2 immunoglobulin[22] (pooled COVID-19 convalescent plasma) using wild type spike RBD (blue), Delta spike RBD (green), or Omicron spike RBD (red) as antigens. The shaded gray region of the plot indicates the area where antibody concentration is less than $K_D/2$ such that binding is not able to exceed 50%.

Figure 3 collates 74 MAAP results performed by us or our collaborators using samples of COVID-19 convalescent serum or plasma from unvaccinated individuals and wild type RBD as the antigen (see Table S3 for details). As shown previously[19], both affinity and concentration of antibodies vary over several orders of magnitude among individuals. However, 75% of samples contained antibodies with K_D values ≤10 nM and total binding site concentrations ≤150 nM (Figure 3). Both casirivimab and imdevimab are derived from convalescent individuals that had been exposed to wild type RBD early in the pandemic[21]. As might be expected, the affinity of casirivimab, which has a competitive mode of action, for wild type RBD is tighter than the majority of the population's response to the same antigen. The non-competitive Imdevimab shows an affinity that is lower than those measured for convalescents. Polyclonal anti-wild type RBD antibodies constitute a mixture of non-neutralizing and neutralizing antibodies (NAbs), with NAbs varying in their neutralization mechanisms[4,25–27]. Regardless of their mechanisms, loss of NAb binding affinity correlates with viral immune escape[25–27], as RBD binding is a pre-requisite for neutralization. In addition to the NAb affinity, the degree to which NAbs bind is determined by the viral load (i.e., the antigen concentration) and the NAb concentration. With reduced affinity, higher NAb concentrations are required to achieve the same levels of binding for a given viral load. If the affinity is too low, even very high NAb concentrations are not sufficient to achieve considerable binding. Since 60% of anti-RBD antibodies isolated from convalescent individuals showed neutralization[27], a reduction in the average affinity of a polyclonal NAb mixture is likely linked to reduced virus neutralization. While imdevimab did not bind to Omicron spike RBD, the affinity of casirivimab was considerably lower than affinities of polyclonal serum antibodies from convalescent individuals, consistent with their loss of virus neutralization ability.

We also assessed how the antibody affinity and the binding site concentration in a pooled convalescent standard plasma responds to Omicron spike RBD. For this experiment, we performed MAAP on the working reagent for anti-SARS-CoV-2 immunoglobulin, which is pooled plasma from COVID-19 convalescent individuals collected between April and May 2020[22]. Antibody affinities and binding site concentrations against wild type RBD were well within the range observed for most of the individual samples (Figure 3).

When challenged with Delta spike RBD, the affinity of antibodies in the pooled plasma decreased slightly by a factor of approximately 1.5 while the concentration of binding sites remained largely unchanged. Surprisingly, against Omicron spike RBD the antibody affinity and concentration were reduced by factors of just 2.5 and 2.0, respectively, compared to wild type. The binding site concentration is still 2-fold higher than K_D suggesting that these polyclonal antibody mixtures retain binding capabilities against Omicron spike RBD. This observation is in line with reports that a considerable population retain some degree of Omicron neutralization after infection with wild type or Alpha strains[8]. During infection, highly neutralizing antibodies with high affinity arise very quickly, such that just 2 mutations from germline can boost affinity 100-fold. However, the vast majority of induced antibodies against SARS-CoV-2 remain near-germline and thus can be more promiscuous for epitope mutations[25–27]. Figure 3 shows that compared with the therapeutic monoclonal antibodies, most individual sera and plasmas have rather low affinity and only very few demonstrate picomolar affinities. For such moderate affinity antibodies, a drop in affinity due to epitope changes will be less profound than for antibodies with high affinity. For the latter, epitope mutation can be detrimental as evidenced by the profoundly reduced affinities of casirivimab and imdevimab.

Conclusions

Using microfluidic diffusional sizing, we quantified the binding affinities of two therapeutic antibodies, casirivimab and imdevimab, to spike receptor binding domains of the wild type variant, the Delta variant, and the Omicron variant. The affinity of casirivimab to Omicron spike RBD was reduced by several orders of magnitude, and imdevimab did not show any binding in our assay. These findings agree with published reports of both antibodies showing high neutralization activity against wild type and Delta, whereas the Omicron variant escapes neutralization by casirivimab and imdevimab. We also find a considerable degree of Omicron spike RBD cross-reactive antibodies in pooled convalescent plasma from 2020. Microfluidic antibody affinity profiling of samples from COVID-19 convalescent individuals provide context to these findings as the average affinities of RBD specific polyclonal antibodies in these samples were not as high as for typical monoclonal therapeutics, rendering the immune response more robust against epitope mutations.

Materials and Methods

Spike RBD reagents

Protein name	SARS-CoV-2 variant	Pango lineage	Vendor	Article number	Amino-acid sequence	Tags	Mutated amino-acid residues
Wild type spike RBD	Wuhan-Hu-1 sequence (NC_045512)	A	Sino Biological	40592-V08H	R319-F541	C-His	
Delta spike RBD	Delta	B.1.617.2	Sino Biological	40592-V08H90	R319-F541	C-His	L452R, T478K
Omicron spike RBD	Omicron	B.1.1.529	Sino Biological	40592-V08H121	R319-F541	C-His	G339D, S371L, S373P, S375F, K417N, N440K, G446S, S477N, T478K, E484A, Q493R, G496S, Q498R, N501Y, Y505H

Antibody reagents

Antibody name	Alternative name	Vendor	Article number
casirivimab	REGN10933	ProteoGenix	PTXCOV-A552
imdevimab	REGN10987	ProteoGenix	PTXCOV-A553

Sample collection, ethics, and biosafety

All plasma and serum samples were collected from unvaccinated convalescent individuals. Unless otherwise stated, no information regarding the application of therapeutic antibodies, immunosuppressant drugs or other therapeutic agents was available for the purposes of this study. All such sample collection was performed in accordance with one of the following:

For all samples[19,28,29] collected by University Hospital Zurich:

All experiments and analyses involving samples from human donors were conducted with the approval of the local ethics committee (KEK-ZH-Nr.2015-0561, BASEC-Nr. 2018-01042, and BASEC-Nr. 2020-01731), in accordance with the provisions of the Declaration of Helsinki and the Good Clinical Practice guidelines of the International Conference on Harmonisation.

EDTA plasma from healthy donors and from convalescent individuals was obtained from the Blutspendedienst (BDS) Kanton Zürich from donors who signed the consent that their samples can be used for conducting research. Samples from patients with COVID-19 were collected at the University Hospital Zurich from patients who signed an informed consent.

For all samples collected by the Fred Hutchinson Cancer Research Center and the University of Washington:

Informed consent was obtained from all human subjects. Plasma samples from SARS-CoV-2 seropositive individuals were obtained from a Fred Hutchinson Cancer Research Center repository and from the repository of the University of Washington. FHCRC repository was assembled from a COVID-19 seroepidemiology study conducted in a single county in the western US and the study was approved by the FHCRC institutional review board (#10453)[30]. UW repository was formed from Seattle-area participants recruited for potential donation of single-donor plasma units (ClinicalTrials.gov: NCT04338360), and plasma for manufacture of a pooled anti–SARS-CoV-2 product (NCT04344977)[31]providing rationale for administration of plasma containing SARS-CoV-2.neutralizing antibodies (nAbs.

For all samples purchased from BioIVT, LLC:

BioIVT sought informed consent from each subject, or the subjects legally authorized representative, and appropriately documented this in writing. All samples are collected under IRB-approved protocols.

For all samples collected by Mayo Clinic:

Samples were residual waste specimens, which were fully de-identified, and thus were used without an IRB.

Fluorescent labeling of proteins

Recombinant proteins were labeled with Alexa Fluor™ 647 NHS ester (Thermo Fisher) as described previously[17]. In brief, solution containing 150 µg of spike RBD was mixed with dye at a three-fold molar excess in the presence of $NaHCO_3$ (Merck) buffer at pH 8.3 and incubated at 4 °C overnight. Unbound label was removed by size-exclusion chromatography (SEC) on an ÄKTA pure system (Cytiva) using a Superdex 75 Increase 10/300 column (Cytiva). Labeled and purified proteins were stored at −80 °C in PBS pH 7.4 containing 10% (w/v) glycerol as cryoprotectant.

Equilibrium binding measurements by microfluidic diffusional sizing (MDS)

Binding affinity of antibodies and spike RBD proteins was measured on a Fluidity One-M (Fluidic Analytics). Fluorescently labeled RBD at a concentration of 1 nM was mixed with unlabelled antibody at 8 different, decreasing concentrations of a three-fold dilution series and incubated on ice for at least 1 hour. PBS-Tween 20 (0.05%) pH 7.5 was used as a dilution buffer. Before the measurement, 3.5 µL of PBS-Tween 20 (0.05%) pH 7.5 was transferred to each of the 24 flow buffer ports of the Fluidity-One M chip plate, and the microfluidic circuits were allowed to prime for at least 1 minute. Then, 3 times 3.5 µL of the 8 different RBD–antibody mixtures were transferred to the 24 sample ports of the Fluidity One-M chip plate to measure a binding curve of 8 antibody concentrations in triplicate. On the Fluidity One-M, the Alexa-647 detection setting and size-range setting of 3 – 14 nm was used. K_D values were determined by non-linear least squares fitting as described previously[17] using Prism (GraphPad Software).

Microfluidic Antibody Affinity Profiling (MAAP) on the working reagent for anti-SARS-CoV-2 immunoglobulin

The working reagent for anti-SARS-CoV-2 immunoglobulin (National Institute for Biological Standards and Control 21/234) is a calibrated product equivalent to the high concentration sample (NIBSC 20/150) from the WHO working standard for anti-SARS-CoV-2 immunoglobulin (NIBSC 20/268). NIBSC 21/234 consist of pooled plasma from individuals who recovered from COVID-19 and was collected between April and May 2020[22]. MAAP was performed as described previously[18–20]. In brief, fluorescently labelled spike RBD from wild type, Delta, and Omicron was mixed with various dilutions of convalescent plasma and incubated on ice for at least 30 min. A buffer containing PBS at pH 7.4, 10% glycerol, and 5% (w/v) human serum albumin was used for plasma dilutions. Equilibrium binding of RBD to plasma antibodies was assessed by monitoring hydrodynamic radii (R_h) on the Fluidity One-M. The measurement protocol was the same as for purified proteins measured in buffer, with the only difference being that 3.5 µL of the plasma sample instead of PBS-Tween (0.05%) was added to the flow buffer ports of the Fluidity One-M chip plate. Bayesian inference was used to determine K_D and binding site concentrations from the mode of the joint posterior distribution, also as described previously[18–20].

Funding Acknowledgements

Institutional core funding by the University of Zurich and the University Hospital of Zurich, as well as Driver Grant 2017DRI17 of the Swiss Personalized Health Network to A.A; funding by grants of Innovation Fund of the University Hospital Zurich (INOV00096), and of the NOMIS Foundation, the Schwyzer Winiker Stiftung, and the Baugarten Stiftung (coordinated by the USZ Foundation, USZF27101) to A.A. and M.E. V.K. was funded by an NIHR fellowship (PD-2016-09-065). T.P.J.K. is grateful for financial support by the Biotechnology and Biological Sciences Research Council and the European Research Council.

Author Contributions

S. Fiedler: conceptualization, data curation, formal analysis, supervision, investigation, visualization, methodology, project administration and writing – original draft, review and editing.

S.R.A. Devenish: conceptualization, data curation, formal analysis, supervision, investigation, visualization, methodology, project administration and writing – original draft, review and editing.

A.S. Morgunov: conceptualization, data curation, formal analysis, supervision, investigation, visualization, methodology, project administration and writing – original draft, review and editing.

A. Ilsley: data curation and writing – review and editing.

F. Ricci: data curation and writing – review and editing.

M. Emmenegger: data curation and writing –review and editing.

V. Kosmoliaptsis: conceptualization, writing – review.

A. Lagerwaard: data curation, project administration and writing – review.

J.R. Mills: conceptualization, resources, data curation, funding acquisition and writing – review.

A.M. Sholukh: conceptualization, data curation, investigation, visualization, project administration and writing – original draft, review and editing.

A. Aguzzi: conceptualization, resources, supervision, and writing—original draft, review, and editing.

A. Iwasaki: conceptualization, supervision, and writing—original draft, review, and editing.

A.K. Lynn: conceptualization, resources, data curation, visualization, project administration, funding acquisition and writing – review and editing.

T.P.J. Knowles: conceptualization, resources, supervision, funding acquisition, methodology, and writing—original draft, review, and editing.

References

(1) WHO. Classification of Omicron (B.1.1.529): SARS-CoV-2 Variant of Concern https://www.who.int/news/item/26-11-2021-classification-of-omicron-(b.1.1.529)-sars-cov-2-variant-of-concern (accessed Dec 27, 2021).

(2) Karim, S. S. A.; Karim, Q. A. Omicron SARS-CoV-2 Variant: A New Chapter in the COVID-19 Pandemic. *Lancet* **2021**. https://doi.org/10.1016/S0140-6736(21)02758-6

(3) Cameroni, E.; Bowen, J. E.; Rosen, L. E.; Saliba, C.; Zepeda, S. K.; Culap, K.; Pinto, D.; VanBlargan, L. A.; De Marco, A.; di Iulio, J.; Zatta, F.; Kaiser, H.; Noack, J.; Farhat, N.; Czudnochowski, N.; Havenar-Daughton, C.; Sprouse, K. R.; Dillen, J. R.; Powell, A. E.; Chen, A.; Maher, C.; Yin, L.; Sun, D.; Soriaga, L.; Bassi, J.; Silacci-Fregni, C.; Gustafsson, C.; Franko, N. M.; Logue, J.; Iqbal, N. T.; Mazzitelli, I.; Geffner, J.; Grifantini, R.; Chu, H.; Gori, A.; Riva, A.; Giannini, O.; Ceschi, A.; Ferrari, P.; Cippà, P. E.; Franzetti-Pellanda, A.; Garzoni, C.; Halfmann, P. J.; Kawaoka, Y.; Hebner, C.; Purcell, L. A.; Piccoli, L.; Pizzuto, M. S.; Walls, A. C.; Diamond, M. S.; Telenti, A.; Virgin, H. W.; Lanzavecchia, A.; Snell, G.; Veesler, D.; Corti, D. Broadly Neutralizing Antibodies Overcome SARS-CoV-2 Omicron Antigenic Shift. *Nature* **2021**. https://doi.org/10.1038/D41586-021-03825-4.

(4) Cao, Y.; Wang, J.; Jian, F.; Xiao, T.; Song, W.; Yisimayi, A.; Huang, W.; Li, Q.; Wang, P.; An, R.; Wang, J.; Wang, Y.; Niu, X.; Yang, S.; Liang, H.; Sun, H.; Li, T.; Yu, Y.; Cui, Q.; Liu, S.; Yang, X.; Du, S.; Zhang, Z.; Hao, X.; Shao, F.; Jin, R.; Wang, X.; Xiao, J.; Wang, Y.; Xie, X. S. Omicron Escapes the Majority of Existing SARS-CoV-2 Neutralizing Antibodies. *Nature* **2021**. https://doi.org/10.1038/D41586-021-03796-6.

(5) Liu, L.; Iketani, S.; Guo, Y.; Chan, J. F.-W.; Wang, M.; Liu, L.; Luo, Y.; Chu, H.; Huang, Y.; Nair, M. S.; Yu, J.; Chik, K. K.-H.; Yuen, T. T.-T.; Yoon, C.; To, K. K.-W.; Chen, H.; Yin, M. T.; Sobieszczyk, M. E.; Huang, Y.; Wang, H. H.; Sheng, Z.; Yuen, K.-Y.; Ho, D. D. Striking Antibody Evasion Manifested by the Omicron Variant of SARS-CoV-2. *Nature* **2021**. https://doi.org/10.1038/D41586-021-03826-3.

(6) Vanblargan, L. A.; Errico, J. M.; Halfmann, P. J.; Zost, S. J.; Crowe, J. E.; Purcell, L. A.; Kawaoka, Y.; Corti, D.; Fremont, D. H.; Diamond, M. S.; Biotechnology, V.; Louis, S.; Mo, U. An Infectious SARS-CoV-2 B.1.1.529 Omicron Virus Escapes Neutralization by Several Therapeutic Monoclonal Antibodies. *bioRxiv* **2021**. https://doi.org/10.1101/2021.12.15.472828.

(7) Dejnirattisai, W.; Huo, J.; Zhou, D.; Zahradník, J.; Supasa, P.; Liu, C.; Duyvesteyn, H. M. E.; Ginn, H. M.; Mentzer, A. J.; Tuekprakhon, A.; Nutalai, R.; Wang, B.; Dijokaite, A.; Khan, S.; Avinoam, O.; Bahar, M.; Skelly, D.; Adele, S.; Johnson, S. A.; Amini, A.; Ritter, T.; Mason, C.; Dold, C.; Pan, D.; Assadi, S.; Bellass, A.; Omo-Dare, N.; Koeckerling, D.; Flaxman, A.; Jenkin, D.; Aley, P. K.; Voysey, M.; Clemens, S. A. C.; Naveca, F. G.; Nascimento, V.; Nascimento, F.; Costa, C. F. da; Resende, P. C.; Pauvolid-Correa, A.; Siqueira, M. M.; Baillie, V.; Serafin, N.; Ditse, Z.; Silva, K. Da; Madhi, S.; Nunes, M. C.; Malik, T.; Openshaw, P. J.; Baillie, J. K.; Semple, M. G.; Townsend, A. R.; Huang, K.-Y. A.; Tan, T. K.; Carroll, M. W.; Klenerman, P.; Barnes, E.; Dunachie, S. J.; Constantinides, B.; Webster, H.; Crook, D.; Pollard, A. J.; Lambe, T.; consortium, O.; consortium, I.; Paterson, N. G.; Williams, M. A.; Hall, D. R.; Fry, E. E.; Mongkolsapaya, J.; Ren, J.; Schreiber, G.; Stuart, D. I.; Screaton, G. R. Omicron-B.1.1.529 Leads to Widespread Escape from Neutralizing Antibody Responses. *bioRxiv* **2021**. 2021.12.03.471045. https://doi.org/10.1101/2021.12.03.471045.

(8) Planas, D.; Saunders, N.; Maes, P.; Guivel-Benhassine, F.; Planchais, C.; Buchrieser, J.; Bolland, W.-H.; Porrot, F.; Staropoli, I.; Lemoine, F.; Péré, H.; Veyer, D.; Puech, J.; Rodary, J.; Baela, G.; Dellicour, S.; Raymenants, J.; Gorissen, S.; Geenen, C.; Vanmechelen, B.; Wawina-Bokalanga, T.; Martí-Carrerasi, J.; Cuypers, L.; Sève, A.; Hocqueloux, L.; Prazuck, T.; Rey, F.; Simon-Lorrière, E.; Bruel, T.; Mouquet, H.; André, E.; Schwartz, O. Considerable Escape of SARS-CoV-2 Omicron to Antibody Neutralization. *Nature* **2021**. https://doi.org/10.1038/D41586-021-03827-2.

(9) Dejnirattisai, W.; Shaw, R. H.; Supasa, P.; Liu, C.; Stuart, A. S.; Pollard, A. J.; Liu, X.; Lambe, T.; Crook, D.; Stuart, D. I.; Mongkolsapaya, J.; Nguyen-Van-Tam, J. S.; Snape, M. D.; Screaton, G. R.; group, study. Reduced Neutralisation of SARS-CoV-2 Omicron B.1.1.529 Variant by Post-Immunisation Serum. *Lancet* **2021**. https://doi.org/10.1016/S0140-6736(21)02844-0.

(10) Lu, L.; Mok, B. W.-Y.; Chen, L.; Chan, J. M.-C.; Tsang, O. T.-Y.; Lam, B. H.-S.; Chuang, V. W.-M.; Chu, A. W.-H.; Chan, W.-M.; Ip, J. D.; Chan, B. P.-C.; Zhang, R.; Yip, C. C.-Y.; Cheng, V. C.-C.; Chan, K.-H.; Hung, I. F.-N.; Yuen, K.-Y.; Chen, H.; To, K. K.-W. Neutralization of SARS-CoV-2 Omicron Variant by Sera from BNT162b2 or Coronavac Vaccine Recipients. *medRxiv* **2021**. https://doi.org/10.1101/2021.12.13.21267668.

(11) Bentley, E. G.; Kirby, A.; Sharma, P.; Kipar, A.; Mega, D. F.; Bramwell, C.; Penrice-Randal, R.; Prince, T.; Brown, J. C.; Zhou, J.; Screaton, G. R.; Barclay, W. S.; Owen, A.; Hiscox, J. A.; Stewart, J. P. SARS-CoV-2 Omicron-B.1.1.529 Variant Leads to Less Severe Disease than Pango B and Delta Variants Strains in a Mouse Model of Severe COVID-19. *bioRxiv* **2021**. https://doi.org/10.1101/2021.12.26.474085.

(12) Abdelnabi, R.; Foo, C. S.; Zhang, X.; Lemmens, V.; Maes, P.; Slechten, B.; André, E.; Weynand, B.; Dallemier, K.; Neyts, J. The Omicron (B.1.1.529) SARS-CoV-2 Variant of Concern Does Not Readily Infect Syrian Hamsters 1. *bioRxiv* **2021** https://doi.org/10.1101/2021.12.24.474086

(13) Diamond, M.; Halfmann, P.; Iwatsuki-Horimoto, K.; Iida, S.; Kiso, M.; Scheaffer, S.; Joshi, A.; Loeber, S.; Ying, B.; Floyd, K. The SARS-CoV-2 B.1.1.529 Omicron Virus Causes Attenuated Infection and Disease in Mice and Hamsters. *Under Review* **2021**. https://doi.org/10.21203/RS.3.RS-1211792/V1.

(14) Wolter, N.; Jassat, W.; Walaza, S.; Welch, R.; Moultrie, H.; Groome, M.; Amoako, D. G.; Everatt, J.; Bhiman, J. N.; Scheepers, C.; Tebeila, N.; Chiwandire, N.; Plessis, M. du; Govender, N.; Ismail, A.; Glass, A.; Mlisana, K.; Stevens, W.; Treurnicht, F. K.; Makatini, Z.; Hsiao, N.; Parboosing, R.; Wadula, J.; Hussey, H.; Davies, M.-A.; Boulle, A.; Gottberg, A. von; Cohen, C. Early Assessment of the Clinical Severity of the SARS-CoV-2 Omicron Variant in South Africa. *medRxiv* **2021**, 2021.12.21.21268116. https://doi.org/10.1101/2021.12.21.21268116.

(15) Meng, B.; ATM Ferreira, I.; Abdullahi, A.; Saito, A.; Kimura, I.; Yamasoba, D.; Kemp, S. A.; Goonawardane, N.; Papa, G.; Fatihi, S.; Rathore, S.; Ikeda, T.; Toyoda, M.; Seng Tan, T.; Kuramochi, J.; Mitsunaga, S.; Ueno, T.; Smith, K. G.; Bradley, J.; Choi, J.; Madissoon, E.; Meyer, K.; Mlcochova, P.; Doffinger, R.; Teichmann, S. A.; James, L.; Hyeon Lee, J.; Thukral, L.; Sato, K.; Gupta, R. K. SARS-CoV-2 Omicron Spike Mediated Immune Escape, Infectivity and Cell-Cell Fusion. *bioRxiv* **2021** https://doi.org/10.1101/2021.12.17.473248.

(16) HKUMed finds Omicron SARS-CoV-2 can infect faster and better than Delta in human bronchus but with less severe infection in lung - News | HKUMed http://www.med.hku.hk/en/news/press/20211215-omicron-sars-cov-2-infection (accessed Jan 2, 2022).

(17) Fiedler, S.; Piziorska, M. A.; Denninger, V.; Morgunov, A. S.; Ilsley, A.; Malik, A. Y.; Schneider, M. M.; Devenish, S. R. A.; Meisl, G.; Kosmoliaptsis, V.; Aguzzi, A.; Fiegler, H.; Knowles, T. P. J. Antibody Affinity Governs the Inhibition of SARS-CoV-2 Spike/ACE2 Binding in Patient Serum. *ACS Infect. Dis.* **2021**. https://doi.org/10.1021/acsinfecdis.1c00047.

(18) Schneider, M. M.; Scheidt, T.; Priddey, A. J.; Xu, C. K.; Hu, M.; Devenish, S. R. A.; Meisl, G.; Dobson, C. M.; Kosmoliaptsis, V.; Knowles, T. P. J. Microfluidic Antibody Affinity Profiling for In-Solution Characterisation of Alloantibody - HLA Interactions in Human Serum. *bioRxiv* **2020**. https://doi.org/10.1101/2020.09.14.296442.

(19) Schneider, M. M.; Emmenegger, M.; Xu, C. K.; Morales, I. C.; Meisl, G.; Turelli, P.; Zografou, C.; Zimmermann, M. R.; Frey, B. M.; Fiedler, S.; Denninger, V.; Jacquat, R. P.; Madrigal, L.; Ilsley, A.; Kosmoliaptsis, V.; Fiegler, H.; Trono, D.; Knowles, T. P.; Aguzzi, A. Microfluidic Characterisation Reveals Broad Range of SARS-CoV-2 Antibody Affinity in Human Plasma. *Life Sci. Alliance* **2022**. https://doi.org/10.26508/LSA.202101270.

(20) Denninger[1], V.; Xu[2], C. K.; Meisl[2], G.; Morgunov[1], A. S.; Fiedler[1], S.; Ilsley[1], A.; Emmenegger[3], M.; Malik[1], A. Y.; Piziorska[1], M. A.; Schneider[2], M. M.; Devenish[1], S. R. A.; Kosmoliaptsis[4], V.; Aguzzi[3], A.; Fiegler[1], H.; Knowles[1], T. P. J. Understanding the Role of Memory Re-Activation and Cross-Reactivity in the Defense against SARS-CoV-2. *bioRxiv* **2021**. https://doi.org/10.1101/2021.07.23.453352.

(21) Hansen, J.; Baum, A.; Pascal, K. E.; Russo, V.; Giordano, S.; Wloga, E.; Fulton, B. O.; Yan, Y.; Koon, K.; Patel, K.; Chung, K. M.; Hermann, A.; Ullman, E.; Cruz, J.; Rafique, A.; Huang, T.; Fairhurst, J.; Libertiny, C.; Malbec, M.; Lee, W. Y.; Welsh, R.; Farr, G.; Pennington, S.; Deshpande, D.; Cheng, J.; Watty, A.; Bouffard, P.; Babb, R.; Levenkova, N.; Chen, C.; Zhang, B.; Hernandez, A. R.; Saotome, K.; Zhou, Y.; Franklin, M.; Sivapalasingam, S.; Lye, D. C.; Weston, S.; Logue, J.; Haupt, R.; Frieman, M.; Chen, G.; Olson, W.; Murphy, A. J.; Stahl, N.; Yancopoulos, G. D.; Kyratsous, C. A. Studies in Humanized Mice and Convalescent Humans Yield a SARS-CoV-2 Antibody Cocktail. *Science* **2020**. *https://doi.org/10.1126/science.abd0827*.

(22) Mattiuzzo, G.; Bentley, E. M.; Hassall, M.; Routley, S.; Richardson, S.; Bernasconi, V.; Kristiansen, P.; Harvala, H.; Roberts, D.; Semple, M. G.; Cw Turtle, L.; Openshaw, P. J.; Baillie, K.; Sofie, L.; Nissen-Meyer, H.; Broch Brantsaeter, A.; Baxendale, H.; Atkinson, E.; Rigsby, P.; Padley, D.; Almond, N.; Rose, N. J.; Page, M. Establishment of the WHO International Standard and Reference Panel for Anti-SARS-CoV-2 Antibody on Behalf of the ISARIC4C Investigators. *WHO* **2020**.

(23) Planas, D.; Veyer, D.; Baidaliuk, A.; Staropoli, I.; Guivel-Benhassine, F.; Rajah, M. M.; Planchais, C.; Porrot, F.; Robillard, N.; Puech, J.; Prot, M.; Gallais, F.; Gantner, P.; Velay, A.; Le Guen, J.; Kassis-Chikhani, N.; Edriss, D.; Belec, L.; Seve, A.; Courtellemont, L.; Péré, H.; Hocqueloux, L.; Fafi-Kremer, S.; Prazuck, T.; Mouquet, H.; Bruel, T.; Simon-Lorière, E.; Rey, F. A.; Schwartz, O. Reduced Sensitivity of SARS-CoV-2 Variant Delta to Antibody Neutralization. *Nature* **2021**. https://doi.org/10.1038/s41586-021-03777-9.

(24) Weinreich, D. M.; Sivapalasingam, S.; Norton, T.; Ali, S.; Gao, H.; Bhore, R.; Musser, B. J.; Soo, Y.; Rofail, D.; Im, J.; Perry, C.; Pan, C.; Hosain, R.; Mahmood, A.; Davis, J. D.; Turner, K. C.; Hooper, A. T.; Hamilton, J. D.; Baum, A.; Kyratsous, C. A.; Kim, Y.; Cook, A.; Kampman, W.; Kohli, A.; Sachdeva, Y.; Graber, X.; Kowal, B.; DiCioccio, T.; Stahl, N.; Lipsich, L.; Braunstein, N.; Herman, G.; Yancopoulos, G. D. REGN-COV2, a Neutralizing Antibody Cocktail, in Outpatients with Covid-19. *N. Engl. J. Med.* **2021**. DOI: 10.1056/NEJMoa2035002.

(25) Barnes, C. O.; Jette, C. A.; Abernathy, M. E.; Dam, K.-M. A.; Esswein, S. R.; Gristick, H. B.; Malyutin, A. G.; Sharaf, N. G.; Huey-Tubman, K. E.; Lee, Y. E.; Robbiani, D. F.; Nussenzweig, M. C.; West, A. P.; Bjorkman, P. J. SARS-CoV-2 Neutralizing Antibody Structures Inform Therapeutic Strategies. **2020**. https://doi.org/10.1038/s41586-020-2852-1.

(26) Yuan, M.; Huang, D.; Lee, C. C. D.; Wu, N. C.; Jackson, A. M.; Zhu, X.; Liu, H.; Peng, L.; van Gils, M. J.; Sanders, R. W.; Burton, D. R.; Reincke, S. M.; Prüss, H.; Kreye, J.; Nemazee, D.; Ward, A. B.; Wilson, I. A. Structural and Functional Ramifications of Antigenic Drift in Recent SARS-CoV-2 Variants. *Science* **2021**. *https://doi.org/10.1126/SCIENCE.ABH1139*.

(27) Dejnirattisai, W.; Zhou, D.; Ginn, H. M.; Duyvesteyn, H. M. E.; Supasa, P.; Case, J. B.; Zhao, Y.; Walter, T. S.; Mentzer, A. J.; Liu, C.; Wang, B.; Paesen, G. C.; Slon-Campos, J.; López-Camacho, C.; Kafai, N. M.; Bailey, A. L.; Chen, R. E.; Ying, B.; Thompson, C.; Bolton, J.; Fyfe, A.; Gupta, S.; Tan, T. K.; Gilbert-Jaramillo, J.; James, W.; Knight, M.; Carroll, M. W.; Skelly, D.; Dold, C.; Peng, Y.; Levin, R.; Dong, T.; Pollard, A. J.; Knight, J. C.; Klenerman, P.; Temperton, N.; Hall, D. R.; Williams, M. A.; Paterson, N. G.; Bertram, F. K. R.; Siebert, C. A.; Clare, D. K.; Howe, A.; Radecke, J.; Song, Y.; Townsend, A. R.; Huang, K. Y. A.; Fry, E. E.; Mongkolsapaya, J.; Diamond, M. S.; Ren, J.; Stuart, D. I.; Screaton, G. R. The Antigenic Anatomy of SARS-CoV-2 Receptor Binding Domain. *Cell* **2021**. https://doi.org/10.1016/J.CELL.2021.02.032.

(28) Emmenegger, M.; De Cecco, E.; Lamparter, D.; Jacquat, R.; Ebner, D.; Schneider, M.; Condado Morales, I.; Schneider, D.; Dogancay, B.; Guo, J.; Wiedmer, A.; Domange, J.; Imeri, M.; Moos, R.; Zografou, C.; Trevisan, C.; Gonzalez-Guerra, A.; Carrella, A.; Dubach, I.; Althaus, C.; Xu, C.; Meisl, G.; Kosmoliaptsis, V.; Malinauskas, T.; Burgess-Brown, N.; Owens, R.; Mongkolsapaya, J.; Hatch, S.; Screaton, G.; Schubert, K.; Huck, J.; Liu, F.; Pojer, F.; Lau, K.; Hacker, D.; Probst-Mueller, E.; Cervia, C.; Nilsson, J.; Boyman, O.; Saleh, L.; Spanaus, K.; von Eckardstein, A.; Schaer, D.; Ban, N.; Tsai, C.-J.; Marino, J.; Schertler, G.; Ebert, N.; Thiel, V.; Gottschalk, J.; Frey, B.; Reimann, R.; Hornemann, S.; Ring, A.; Knowles, T.; Xenarios, I.; Stuart, D.; Aguzzi, A. Early Peak and Rapid Decline of SARS-CoV-2 Seroprevalence in a Swiss Metropolitan Region. *medRxiv* **2020**. https://doi.org/10.1101/2020.05.31.20118554.

(29) Emmenegger, M. I.; Saseendran Kumar, S. I.; Emmenegger, V.; Malinauskas, T. I.; Buettner, T.; Rose, L.; Schierack, P.; Sprinzl, M. F.; Sommer, C. J.; Lackner, K. J.; Aguzzi, A.; Roggenbuck, D. I.; M Frauenknecht ID, K. B. Anti-Prothrombin Autoantibodies Enriched after Infection with SARS-CoV-2 and Influenced by Strength of Antibody Response against SARS-CoV-2 Proteins. *PLOS Pathog.* **2021**. https://doi.org/10.1371/JOURNAL.PPAT.1010118.

(30) McLaughlin, C. C.; Doll, M. K.; Morrison, K. T.; McLaughlin, W. L.; O'Connor, T.; Sholukh, A. M.; Bossard, E. L.; Phasouk, K.; Ford, E. S.; Diem, K.; Klock, A. M.; Jerome, K. R.; Corey, L. High Community SARS-CoV-2 Antibody Seroprevalence in a Ski Resort Community, Blaine County, Idaho, US. Preliminary Results. *medRxiv* **2020**. https://doi.org/10.1101/2020.07.19.20157198.

(31) Boonyaratanakornkit, J.; Morishima, C.; Selke, S.; Zamora, D.; McGuffin, S.; Shapiro, A. E.; Campbell, V. L.; McClurkan, C. L.; Jing, L.; Gross, R.; Liang, J.; Postnikova, E.; Mazur, S.; Lukin, V. V.; Chaudhary, A.; Das, M. K.; Fink, S. L.; Bryan, A.; Greninger, A. L.; Jerome, K. R.; Holbrook, M. R.; Gernsheimer, T. B.; Wener, M. H.; Wald, A.; Koelle, D. M. Clinical, Laboratory, and Temporal Predictors of Neutralizing Antibodies against SARS-CoV-2 among COVID-19 Convalescent Plasma Donor Candidates. *J. Clin. Invest.* **2021**. https://doi.org/10.1172/JCI144930.

(32) Emma B. Hodcroft. CoVariants: SARS-CoV-2 Mutations and Variants of Interest https://covariants.org/.

Supplementary Information

Table S1. Mutations within the spike protein shared among SARS-CoV-2 variants[32].

		SARS-CoV-2 variant										
Spike protein		Alpha	Beta	Gamma	Delta	Kappa	Omicron (BA.1)	Omicron (BA.2)	Eta	Iota	Lambda	Mu
Do-main	Re-gion	Shared mutations										
S1	NTD	L18F	L18F									
					T19R			T19I				
				P26S				P26-				
							A67V		A67V			
		H69-					H69-		H69-			
		V70-					V70-		V70-			
							T95I			T95I		T95I
							G142-	G142-				
							V143-	V143-				
		Y144-					Y144-	Y144-	Y144-			Y144S
							Y145D	Y145D				Y145N
										D253G	D253N	
	RBD						G339D	G339D				
							S371L	S371F				
							S373P	S373P				
							S375F	S375F				
			K417N	K417T			K417N	K417N				
							N440K	N440K				
					L452R	L452R					L452Q	
							S477N	S477N				
					T478K		T478K	T478K				
			E484K	E484K		E484Q	E484A	E484A	E484K	E484K		E484K
							Q493R	Q493R				
							Q498R	Q498R				
		N501Y	N501Y	N501Y			N501Y	N501Y				N501Y
							Y505H	Y505H				
	SD2	D614G	D614G	D614G	D614G	D614G	D614G	D614G	D614G	D614G	D614G	D614G
				H655Y			H655Y	H655Y				
							N679K	N679K				
		P681H			P681R	P681R	P681H	P681H				P681H

S2		A701V								A701V		
							N764K	N764K				
							D796Y	D796Y				
	HR1				D950N							D950N
							Q954H	Q954H				
							N969K	N969K				

Table S2. Mutations within the spike protein unique among SARS-CoV-2 variants[32].

SARS-CoV-2 variant												
		Alpha	**Beta**	**Gamma**	**Delta**	**Kappa**	**Omicron (BA.1)**	**Omicron (BA.2)**	**Eta**	**Lota**	**Lambda**	**Mu**
		Unique mutations										
		A570D	D80A	T20N	E156-	E154K	N211-	L24-	Q52R	L5F	G75V	R346K
		T716I	D215G	D138Y	F157-	Q1071H	L212I	P25-	Q677H		T76I	
		S982A	L241-	R190S	R158G		G446S	A27S	F888L		R246-	
		D1118H	L242-	T1027I			G496S	V213G			S247-	
			A243-	V1176F			T547K	T376A			Y248-	
							N856K	D405N			L249-	
							L981F	R408S			T250-	
											P251-	
											G252-	
											F490S	
											T859N	

Table S3. Summary of unpublished microfluidic antibody affinity profiling data from SARS-CoV-2 convalescent samples shown in Figure 3. Results from samples collected by Blutspendedienst (BDS) Kanton Zürich and University Hospital Zurich (CH) have been published previously in Life Sci. Alliance 2021, 5 (2), e202101270. Results from samples purchased from BioIVT LLC, have been published previously on bioRxiv (doi: 10.1101/2021.07.23.453352 and doi: 10.1101/2021.07.23.453327).

Sample source: Working reagent for anti-SARS-CoV-2 immunoglobulin, NIBSC code 21/234. National Institute for Biological Standards and Control (UK)							
	K_D (nM)				**Antibody concentration (nM)**		
Antigen	**best fit**	**lower 95% CI**	**upper 95% CI**		**best fit**	**upper 95% CI**	**lower 95% CI**
SARS-CoV-2 wt spike RBD	12.3	9.3	16.4		110	130	93.9
SARS-CoV-2 delta spike RBD	17.5	13	24.3		119	138	98.1
SARS-CoV-2 omicron spike RBD	30.1	23	39.9		59.3	71.7	46.4
Sample source: Fred Hutchinson Cancer Research Center, Seattle WA, USA							
	K_D (nM)				**Antibody concentration (nM)**		
Antigen	**best fit**	**lower 95% CI**	**upper 95% CI**		**best fit**	**lower 95% CI**	**upper 95% CI**
SARS-CoV-2 wt spike RBD	11.2	3.2	26.8		246	76.7	452
SARS-CoV-2 wt spike RBD	9.3	4.1	18.9		70.5	40.5	110
SARS-CoV-2 wt spike RBD	6.9	3.6	12.2		676.8	597	813
SARS-CoV-2 wt spike RBD	9.4	5.8	13.2		240	196	281
SARS-CoV-2 wt spike RBD	17.4	12.4	23.1		495	414	583
SARS-CoV-2 wt spike RBD	8.6	3.2	25.9		424	230	777
SARS-CoV-2 wt spike RBD	40.4	23.5	64.9		239	161	324
SARS-CoV-2 wt spike RBD	15.1	0.29	37.0		104	3.1	202
SARS-CoV-2 wt spike RBD	4.5	0.01	11.2		190	67.7	349
SARS-CoV-2 wt spike RBD	10.9	3.9	27.4		170	77.3	275
SARS-CoV-2 wt spike RBD	9.3	0.06	28.5		71.7	22.0	127
SARS-CoV-2 wt spike RBD	5.8	1.9	11.0		140	99.6	192
SARS-CoV-2 wt spike RBD	25.4	11.9	60.9		249	127	400
SARS-CoV-2 wt spike RBD	9.7	0.01	1108		9.7	0.09	1416
SARS-CoV-2 wt spike RBD	9.4	3.4	16.1		1778	1176	2270
SARS-CoV-2 wt spike RBD	30.7	11.8	62.5		275	146	788
SARS-CoV-2 wt spike RBD	6.8	1.4	19.6		26.7	11.3	46
SARS-CoV-2 wt spike RBD	48.3	1.0	278		326	4.5	804
SARS-CoV-2 wt spike RBD	9.2	0.01	294		373	0.0	3441
SARS-CoV-2 wt spike RBD	6.5	2.8	11.7		135	108	178
SARS-CoV-2 wt spike RBD	51.8	20.0	124		340	103	1014
SARS-CoV-2 wt spike RBD	16.3	10.5	24.1		297	224	383
SARS-CoV-2 wt spike RBD	7.4	0.02	14.3		96.0	32.0	151
SARS-CoV-2 wt spike RBD	29.2	17.2	47.7		430	241	583
SARS-CoV-2 wt spike RBD	18.5	8.1	37.7		92.0	39.0	153
Sample source: Mayo Clinic, Rochester, MN, USA							
	K_D (nM)				**Antibody concentration (nM)**		
Antigen	**best fit**	**lower 95% CI**	**upper 95% CI**		**best fit**	**lower 95% CI**	**upper 95% CI**
SARS-CoV-2 wt spike RBD	0.55	0.011	1.5		2.3	1.2	5.6
SARS-CoV-2 wt spike RBD	0.02	0.010	1.98		22.3	14.6	66.5

SARS-CoV-2 wt spike RBD	1.0	0.013	2.8		19.4	13.1	26.2
SARS-CoV-2 wt spike RBD	0.02	0.010	0.67		3.3	2.0	10.4

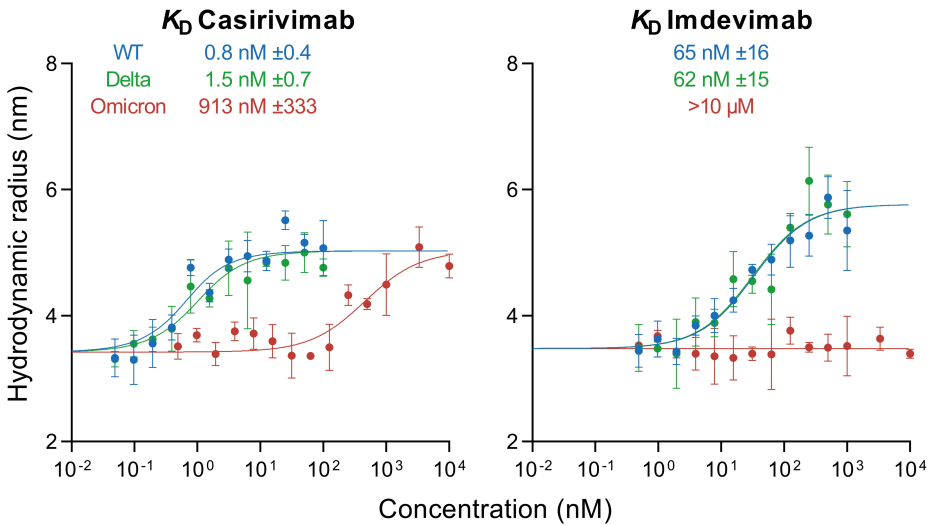
K_D Casirivimab
WT 0.8 nM ±0.4
Delta 1.5 nM ±0.7
Omicron 913 nM ±333
K_D Imdevimab
65 nM ±16
62 nM ±15
>10 μM
Hydrodynamic radius (nm)
8
6
4
2
10^{-2} 10^{-1} 10^{0} 10^{1} 10^{2} 10^{3} 10^{4}
Concentration (nM)

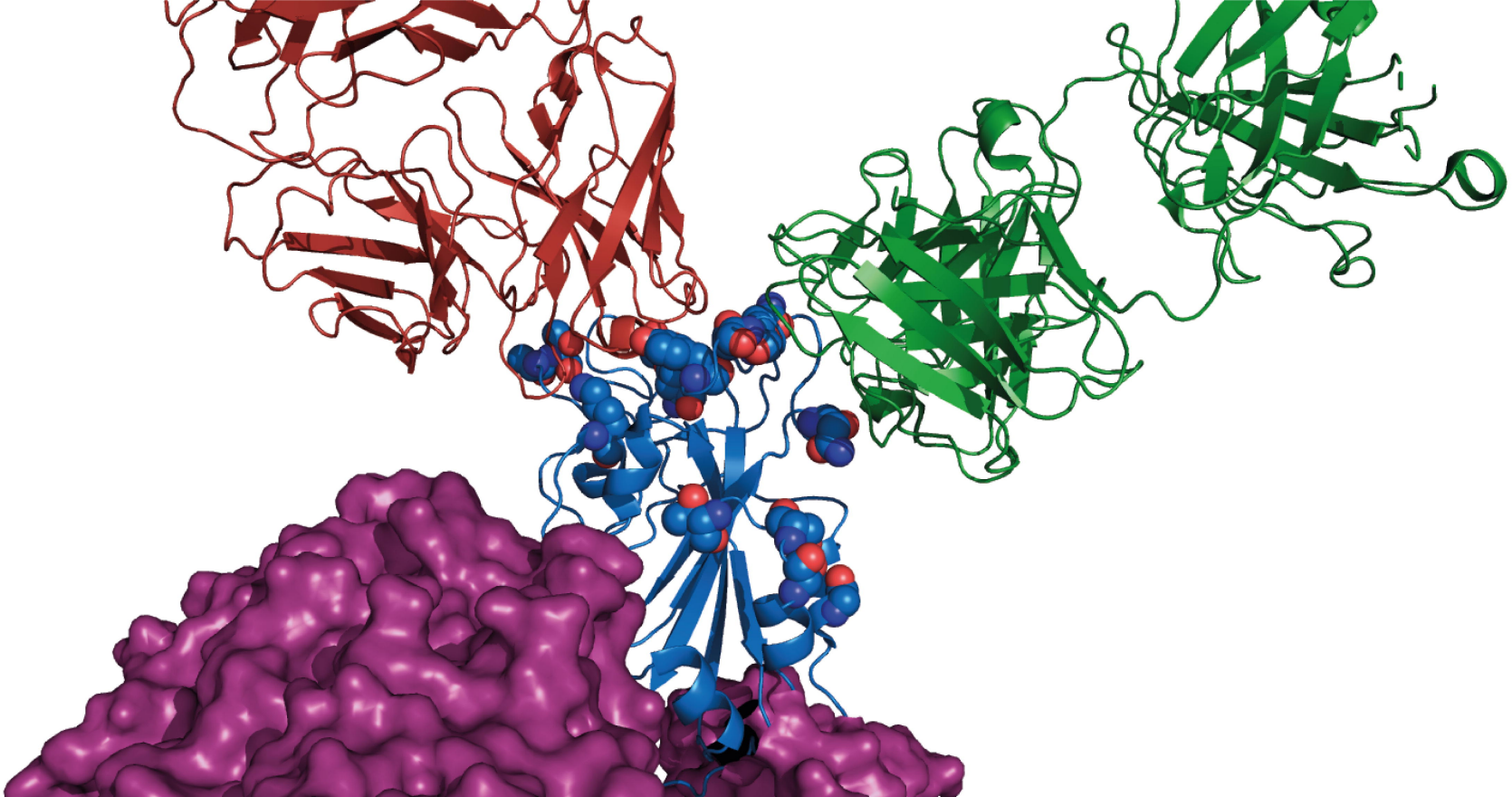

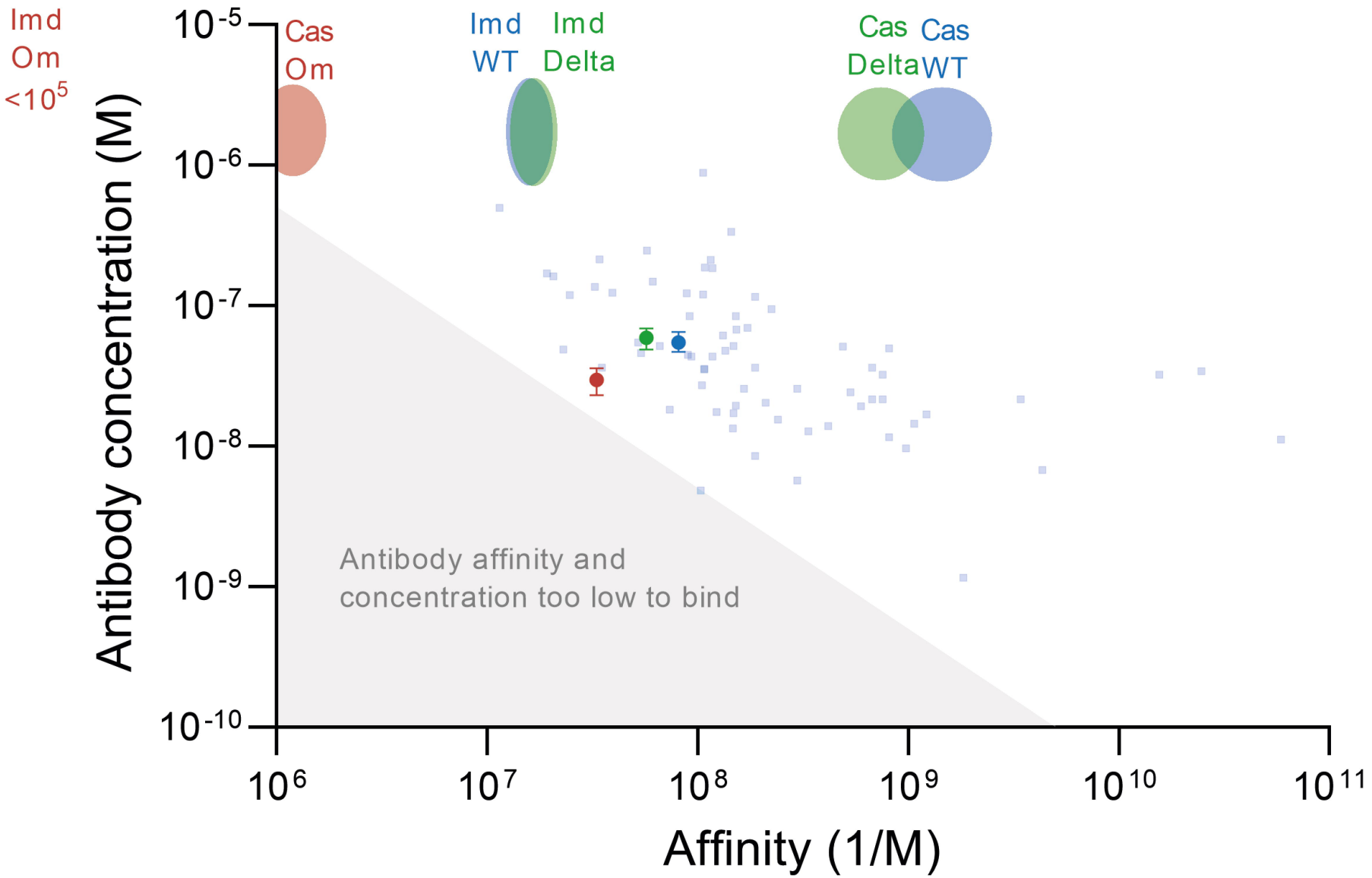
Imd
Om
<10^5
Cas
Om
Imd
WT
Imd
Delta
Cas
Delta
Cas
WT
Antibody concentration (M)
10^-5
10^-6
10^-7
10^-8
10^-9
10^-10
Antibody affinity and
concentration too low to bind
10^6
10^7
10^8
10^9
10^10
10^11
Affinity (1/M)